Supplementary Material

Butterfly wing patterns create powerful illusory motion cues

Real butterfly take-off recordings

Motion energy across frames

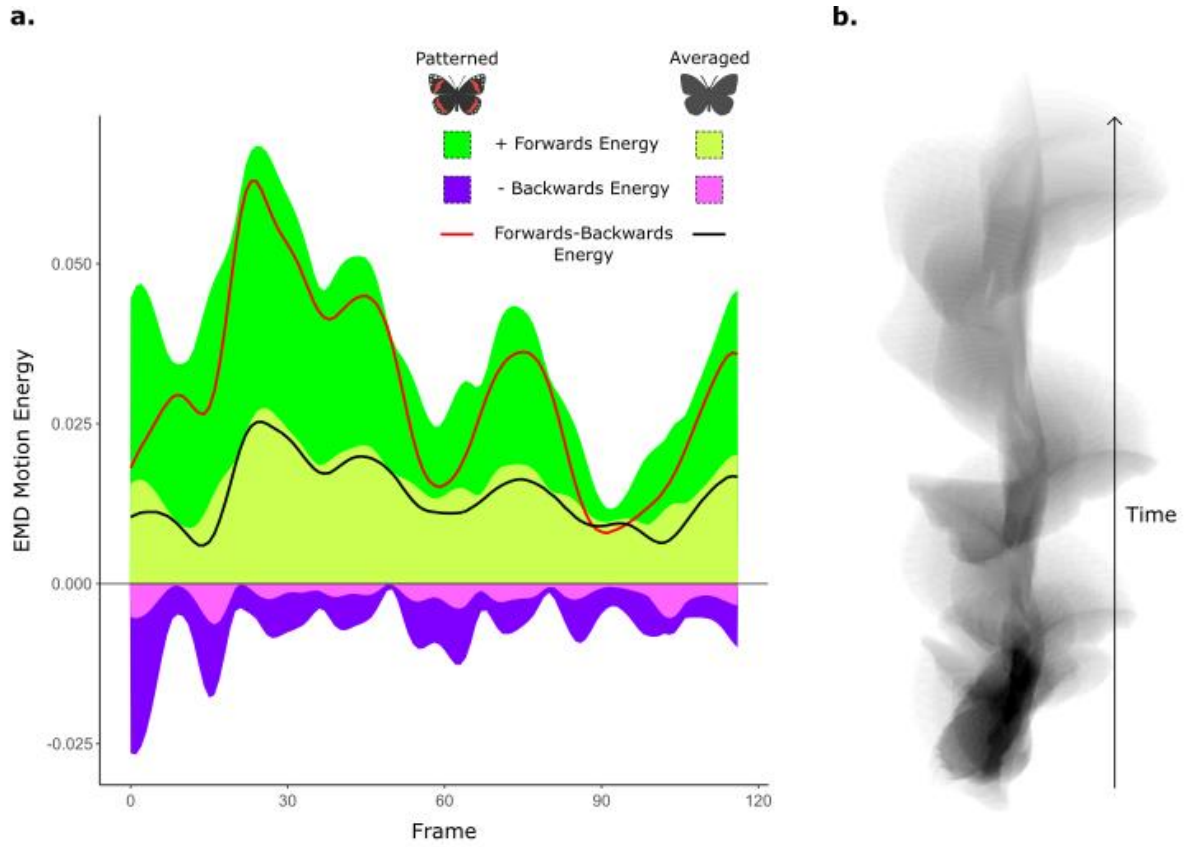

Supplementary Fig.1 | Motion energy and confusion across frames, *a.* example motion forwards and backwards motion energy level for a red admiral, *Vanessa atalanta,* in free flight with is natural patterning and with its patterned averaged. Backwards energy is depicted as negative as it is an opponent to forwards energy. Lines represent the forwards energy subtracted by the backwards energy. The initial peak in forwards and backwards energy represents the point of takeoff for the butterfly and is also when backwards energy is at its highest. Patterning increases the overall energy compared to the unpatterned and increases the ratio of backwards energy in proportion to forwards energy at multiple instances during flight. **b.** Shows the position of the butterfly across time, starting from the bottom, by masking the butterfly for each frame, adding each frame together, and then dividing by the number of frames. Note, as the butterfly does not fly in a straight line forwards and backwards, energy will not always correspond with the heading of the butterfly.

Ratios of energy across directions

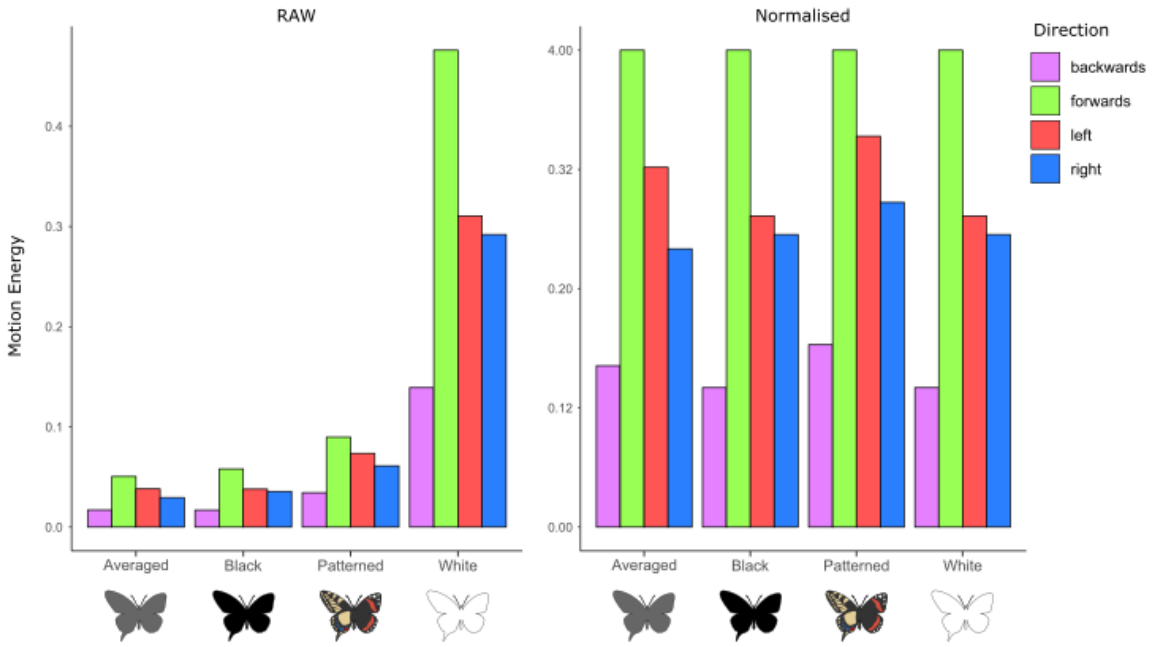

Supplementary Fig.2 | Motion energy ratios, depicts the average motion energy across all frames for all butterfly flights, with the different colour treatments. Energy is split into the four cardinal directions (backwards, forwards, left, and right). The left panel shows the raw average, while the right panel shows the energy divided by the greatest energy value across the four directions. Energy in general is higher for the white treatment compared to other treatments as the white is more contrasting against the background, followed by the patterned. Butterfly wing patterning overall increases the proportion of backwards, left, and right energy compared to forwards.

Influence of patterning on motion confusion metrics

Forwards-Confusion

Supplementary Table 1 | Tukey posthoc test for real butterfly takeoff forwards-confusion

Contrast	Estimate	SE	DF	T ratio	P value
Patterned vs Averaged	0.079	0.007	9350	11.504	<0.001
Patterned vs Black	0.078	0.007	9350	11.478	<0.001
Patterned vs White	0.078	0.007	9350	11.472	<0.001
Averaged vs Black	0	0.007	9350	-0.026	1
Averaged vs White	0	0.007	9350	-0.032	1
Black vs White	0	0.007	9350	-0.006	1

Sideways-Confusion

Supplementary Table 2 | Tukey posthoc test for real butterfly takeoff sideways-confusion

Contrast	Estimate	SE	DF	T ratio	P value
Patterned vs Averaged	0.044	0.005	9352	9.538	<0.001
Patterned vs Black	0.044	0.005	9352	9.538	<0.001
Patterned vs White	0.044	0.005	9352	9.538	<0.001
Averaged vs Black	0	0.005	9352	0.105	1
Averaged vs White	0	0.005	9352	0.104	1
Black vs White	0	0.005	9352	-0.001	1

Forwards-Energy

All butterfly pattern treatments were significantly different from one another for forwards-energy. On average butterflies with a higher contrast against the background (white) have increased forwards-energy. Patterning increases forwards-energy compared to averaged and produces marginally greater forwards energy then black, likely due to the white colours present on the different butterfly species. The averaged butterflies were significantly worse than all other pattern treatments.

Supplementary Table 3 | Tukey posthoc test for real butterfly takeoff forwards-energy

Contrast	Estimate	SE	DF	T ratio	P value
Patterned vs Averaged	0.081	0.004	9362	22.286	<0.001
Patterned vs Black	0.010	0.004	9362	2.629	0.0426
Patterned vs White	-0.415	0.004	9362	-114.567	<0.001
Averaged vs Black	-0.071	0.004	9362	-19.658	<0.001
Averaged vs White	-0.496	0.004	9362	-136.854	<0.001
Black vs White	-0.424	0.004	9362	-117.196	<0.001

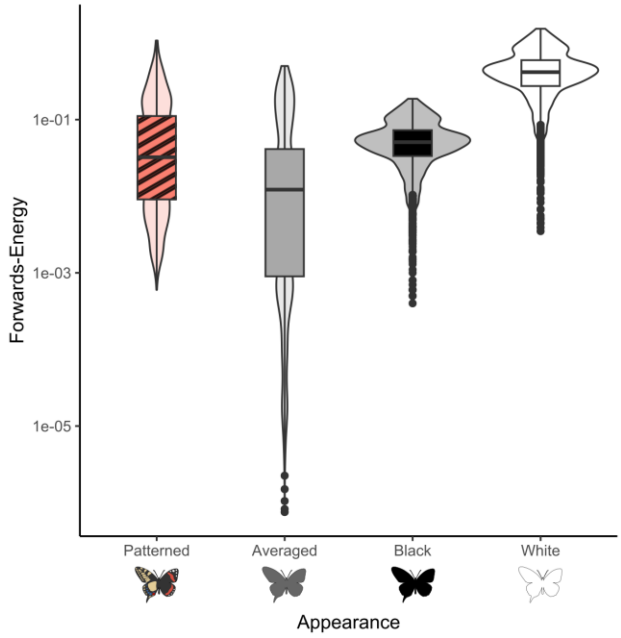

Supplementary Fig.3 | Influence of patterning on forwards-energy, boxplots with violins for forward energy across all frames for all 7 butterfly wing morphotypes with patterning, and without patterning (averaged, black, and white).

Motion confusion across European butterflies

Butterfly phylogeny principal coordinates

For our principal coordinates:

High PCo1 values corresponded with Nymphalids, predominantly Satyrinae, while low values corresponded with Lycaenidae.

High PCo2 values corresponded with Hesperiidae and to a lesser extent Pieridae and Papilonidae, while low values corresponded with Lycanidae and Nymphalidae.

High PCo3 values corresponded with Hesperiidae while low values corresponded with Pieridae. Intermediate values comprised all other families.

See Supplementary Fig. 4 and Fig. 5.

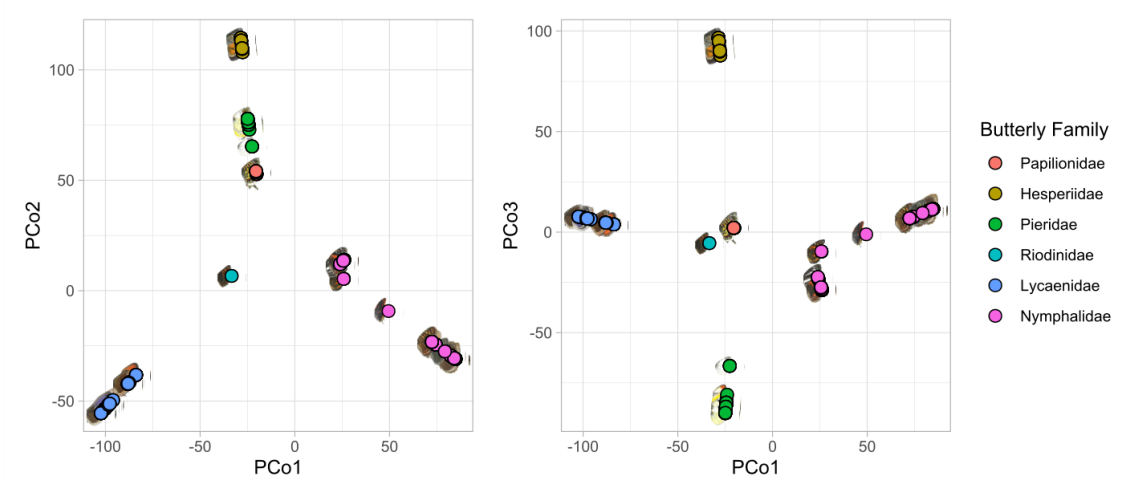

Supplementary Fig.4 | Principal coordinates for European butterflies, plots show the principal coordinates (PCos) for the 6 European butterfly families. The left hand plot shows the positions of PCo1 and PCo2, while the right-hand plot shows PCo1 and PCo3.

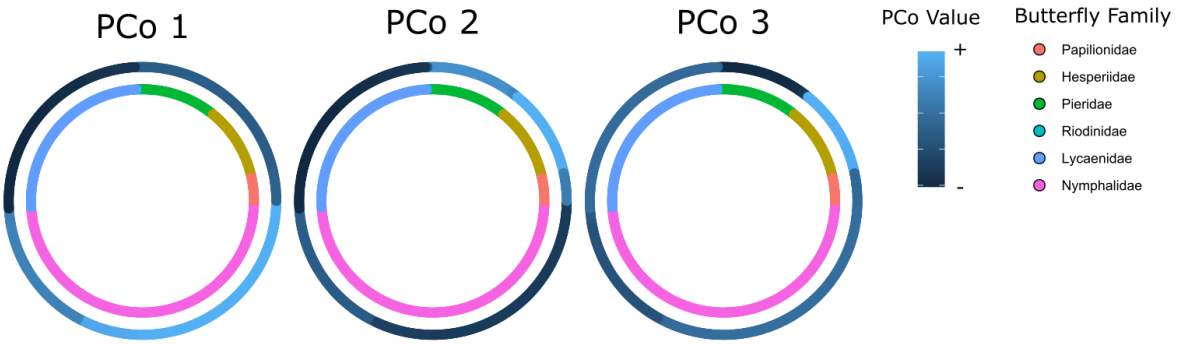

Supplementary Fig.5 | Circular phylogeny of PCo values4, plots show the three principal coordinates (PCos) for the 6 European butterfly families in relation to the shorter phylogeny. Colour values for the inner circle denote the butterfly family and colour values for the outer circle denote the PCo value with lighter blue indicating positive values (+) and darker values denoting negative (-).

Influence of sex on motion confusion metrics

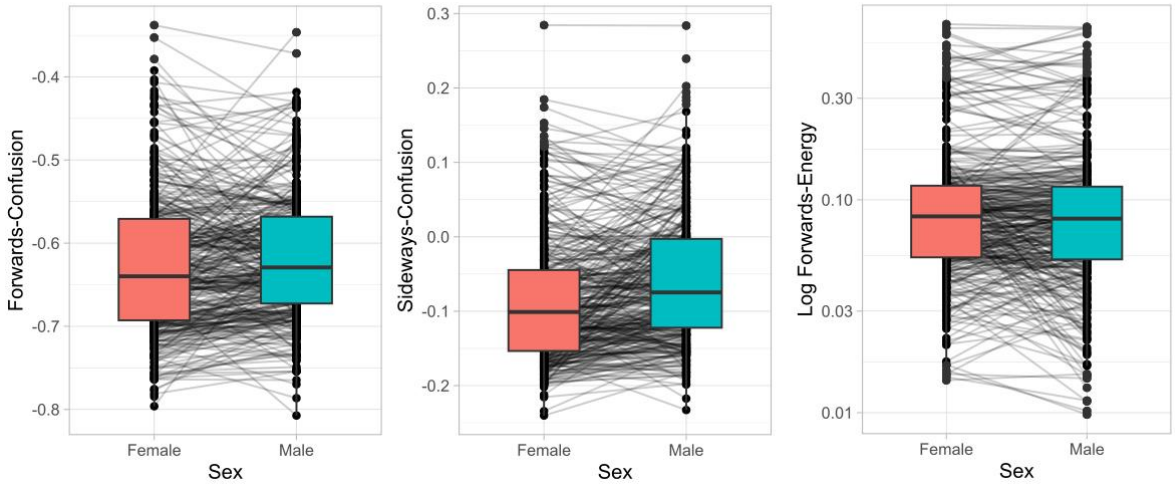

Supplementary Fig.6 | Influence of sex on butterfly motion confusion for flapping flight, each plot shows a boxplot for each of the two sexes and points with lines linking members of the same species.

Given that many butterfly species were illustrated as sexually dimorphic in appearance (358 of our 397 species) and males are frequently more contrasting in appearance than females, we opted to compare our three motion confusion metrics between males and females (See Supplementary Fig.6). To compare each sex we used linear mixed models with the motion confusion metric as the response variable and the sex as the predictor variable with the species binomial as a random effect.

Males were found to have no significant difference in forwards-confusion (male vs female, forwards-confusion: $\beta = 0.006$, $t\ value_{357} = 1.82$, $p = 0.0696$), marginally lower forwards-energy than females (male vs female, forwards-energy: $\beta = -0.057$, $t\ value_{357} = -2.073$, $p = 0.039$), and significantly greater sideways confusion (male vs female, sideways-confusion: $\beta = 0.025$, $t\ value_{357} = 6.49$, $p < 0.001$).

Influence of patterning and gliding on motion confusion metrics

To confirm our results for the influence of patterning on motion confusion in butterflies for the real butterfly takeoffs, we repeated our comparison of motion confusion measures for butterflies with their natural wing patterns and those without their wing patterns (white and averaged wing luminance). Numerous butterfly species, in particular larger species, undergo periods of unpowered flight where the wings are held open in a glide. These periods of differential patterns of biological motion are likely to influence the intensity of motion in

different directions and as a result motion confusion. As our 3D blender model allowed us to render butterfly flights with and without flapping flight we also quantified how wing patterning influenced the EMD when gliding (no flapping).

To compare the effects of patterning and gliding for each motion confusion metric we used linear mixed models. The confusion metric was given as the response variable, and both the pattern treatment (patterned, averaged, or white), the flight method (gliding or flapping) and the interaction between them were used as predictor variables. The unique morphotype of the butterfly was used as a random effect.

As with our real butterflies patterning increased motion confusion compared to the unpatterned treatments, however motion confusion was in some instances higher for the averaged butterflies when the butterflies near perfectly matched the background average (See Supplementary Fig.7 and Table 4-6). Flapping flight was found to be integral to the generation of forwards-confusion effects with the level of backward motion detected being near zero in the absence of wing movement. Meanwhile gliding exacerbated the difference between patterned and the unpatterned treatments for sideways-confusion and increased the level of forward-energy across all treatments (given the reduction in movement in alternative directions),but did not interact with patterning for forward-energy. Outliers for flapping flight where averaged butterflies caused high degrees of forwards and sideways motion confusion were due to instances where the butterflies matched the luminance of the patternless background (See Supplementary Fig. 8).

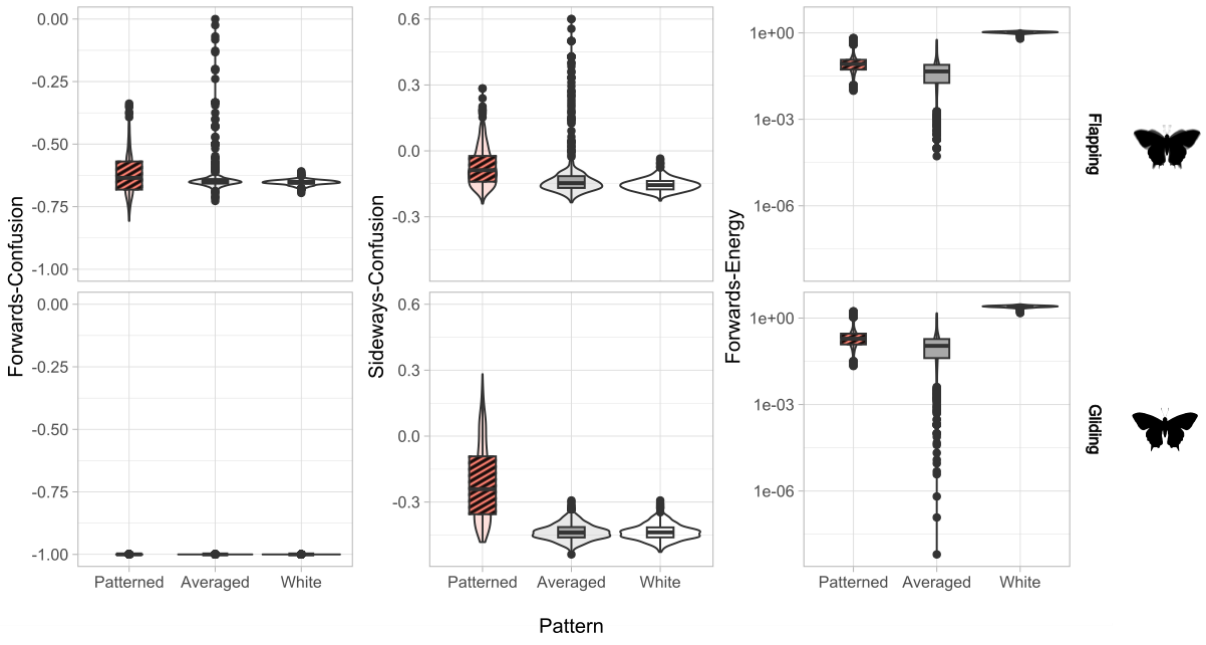

Supplementary Fig.7 | Influence of pattern and gliding on motion confusion metrics, levels of forwards-confusion, sideways-confusion, and forwards-energy for simulated butterfly flight when flapping their wings (above) and when their wings are static (gliding). Butterflies were rendered either with patterns, their averaged luminance or as white.

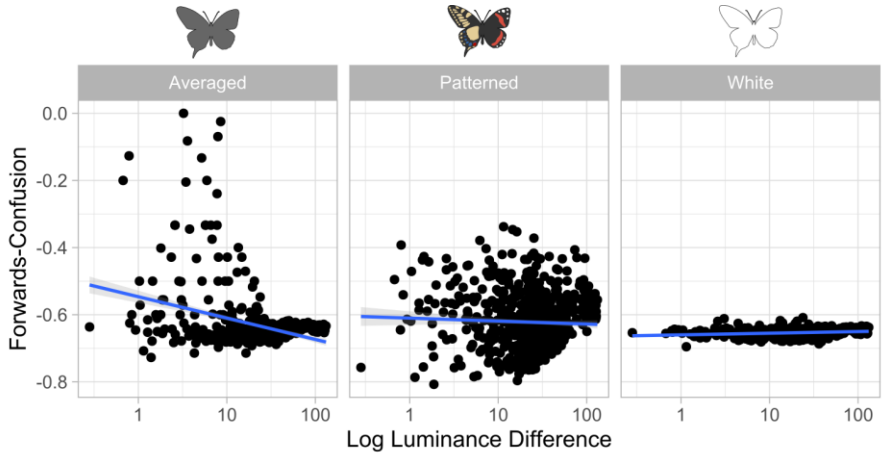

Supplementary Fig.8 | Influence of background match on motion confusion metrics, how does log difference in luminance from the background influence motion confusion for the three pattern treatments, averaged, patterned, and white.

Supplementary Table 4 | Linear mixed model for forwards-confusion, gliding and pattern type

Contrast	Estimate	SE	DF	T ratio	P value
Patterned vs Averaged	-0.012	0.002	3780	-5.217	<0.001
Patterned vs White	-0.031	0.002	3780	-13.739	<0.001
Gliding vs Flapping	-0.378	0.002	3780	-167.952	<0.001
Patterned vs Average : Gliding	0.012	0.002	3780	3.635	<0.001
Patterned vs White : Gliding	0.031	0.002	3780	9.659	<0.001

Supplementary Table 5 | Linear mixed model for sideways-confusion, gliding and pattern type

Contrast	Estimate	SE	DF	T ratio	P value
Patterned vs Averaged	-0.044	0.004	3780	-11.05	<0.001
Patterned vs White	-0.082	0.004	3780	-20.54	<0.001
Gliding vs Flapping	-0.143	0.004	3780	-35.51	<0.001
Patterned vs Average : Gliding	-0.177	0.004	3780	-31.21	<0.001

Patterned vs White : Gliding	-0.140	0.004	3780	-24.55	<0.001

Supplementary Table 6 | Linear mixed model for forwards-energy, gliding and pattern type

Contrast	Estimate	SE	DF	T ratio	P value
Patterned vs Averaged	-0.991	0.046	3780	-21.658	<0.001
Patterned vs White	2.536	0.046	3780	55.412	<0.001
Gliding vs Flapping	0.862	0.046	3780	18.837	<0.001
Patterned vs Average : Gliding	-0.102	0.046	3780	-1.578	0.115
Patterned vs White : Gliding	0.018	0.046	3780	0.282	0.778

Empirical image analysis of butterfly wing patterning

To quantify the appearance of butterfly wings we used image statistics maps for the forewing and hindwing to allow us to measure the mean, standard deviation, x-axis gradient, and y-axis gradient of each statistic. For the gradients a positive gradient indicates an increase in the map's value from left to right / top to bottom of the image, and a negative gradient indicates a decrease. To illustrate how these maps work we provide examples for three butterfly wings (See Supplementary Fig 8). For each map the largest spatial scale, s6, was equivalent to ¼ the square root of the wings area in pixels.

For each butterfly, metrics are split between the forewing and hindwing, e.g. fw.pat.E.mean is the mean energy for the forewing and hw.pat.VH.stdev is the variation in vertical horizontal

orientation for the hindwing. Pat stands for patterning measure and is used to distinguish wing shape measures, .shp.

L = luminance, P =periodicity, VH = vertical-horizontal, OA = obtuse - acute, and DR = directionality.

Luminance map -

Simply created by converting the image from sRGB to blue-tit double cone quantum catch.

Periodicity map -

For each pixel, periodicity is calculated as the weighted average spatial scale (S={s1,s2 ,…,s6}), where each scale is weighted by the absolute value of the difference of gaussian (DoG) output. Higher periodicity (values closer to 1) indicate larger spatial scales.

Px = pixel value

s = scale

wS = $\sum_{s \in S} \frac{abs(px)s}{s}$ = Weighted Sum

E = $\sum_{s \in S} abs(px)s$ = Total Energy

Periodicity = $\frac{wS}{E}$

Energy map -

For each pixel, energy is calculated as the sum absolute value of each pixel across spatial scales (S={s1,s2,…,s6}).

px = pixel value

s = scale

E = $\sum_{s \in S} abs(px)s$ = Total Energy

VH, OA & Directionality maps-

Unlike periodicity and energy, these metrics use Gabor filters at six orientations (0, 30, 60, 90, 120, and 150 degrees) but at the same six spatial scales as the DoG. These orientations are then converted into spatial maps in four different directions by calculating the energy across each orientation.

px = pixel value

a = angle in radians

V (0 degrees) = $\sum_{s \in S} \sin(a) * abs(px)s$

H (90 degrees) = $\sum_{s \in S} \cos(a) * abs(px)s$

A (135 degrees) = $\sum_{s \in S} \sin(a * \frac{\pi}{4}) * abs(px)s$

O (135 degrees) = $\sum_{s \in S} \cos(a * \frac{\pi}{4}) ** abs(px)s$

Then each image (V, H, A, O) is used to create the following image statistics map. VH where each pixel is the value for V - H, OA where each pixel is the value of O - A, and Directionality where each pixel is the value is $\sqrt{(VH^2 + OA^2)}$ - E, with positive values being more directional.

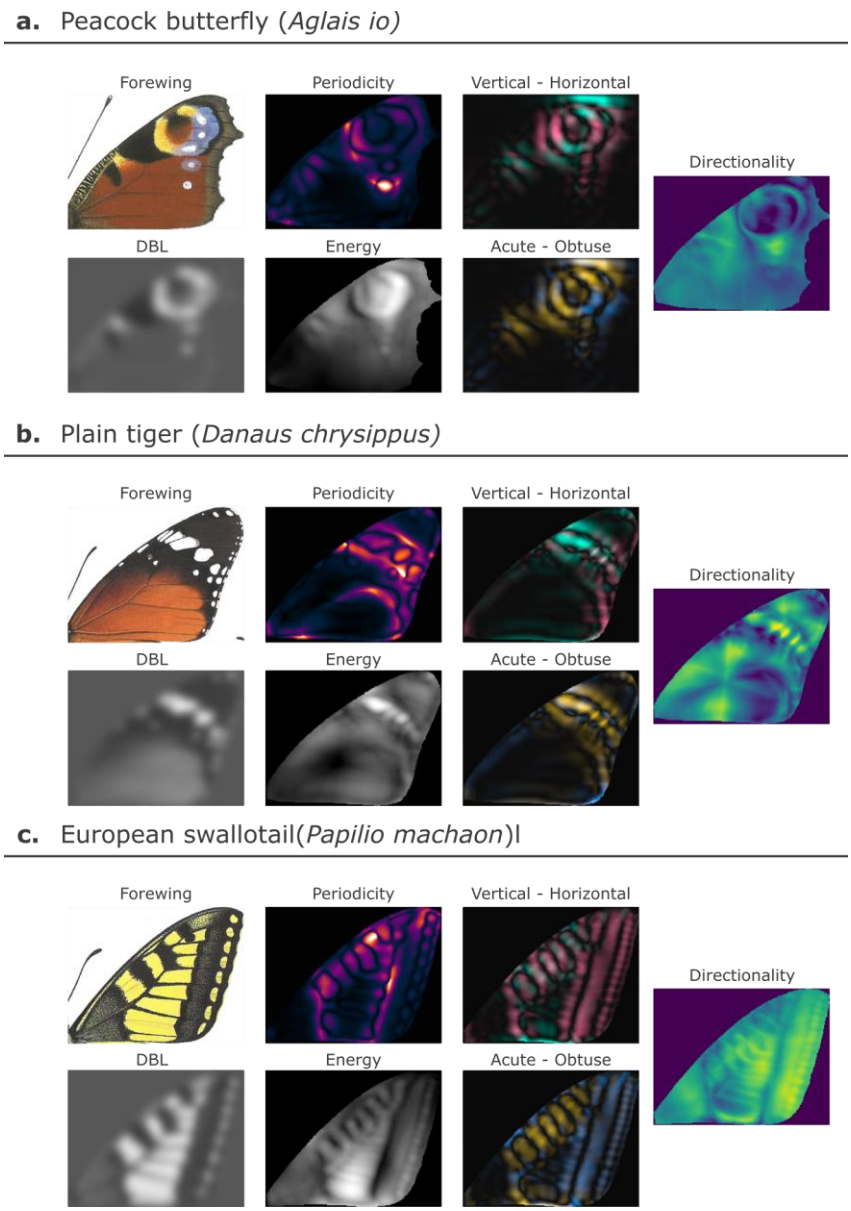

Supplementary Fig.9 | Image statistics maps, example image statistic maps for three different butterfly species. DBL, blue-tit cone catch for the wing downscaled so that the ¼ the wings area was 64 pixels. Lighter values indicate lighter regions. Periodicity, a spatial scale map where brighter values

indicate higher spatial frequencies. Energy, brighter values indicate regions of greater internal contrast from the rest of the wing. Vertical - Horizontal, shows VH where red values are more vertical and green values are more horizontal. Acute - Obtuse, shows OA where yellow values are closer to 135 degrees and blue values are closer to 45 degrees. Directionality, where lighter yellower values indicate more directional patterns.

Random forests for motion confusion metrics

See empirical image analysis of butterflies above for pattern variable denotation. Butterfly phylogeny is given using principal coordinates (PCos) 1-3.

Supplementary Table 7 | SHAP table for forwards-confusion. Variables are ordered by absolute mean SHAP value.

Feature	Node purity	Mean SHAP ± std dev
fw.pat.L.stdev	0.6014	0.0051 ± 0.0109
fw.pat.E.mean	0.6713	0.0046 ± 0.0101
hw.pat.VH.mean	0.3468	0.0042 ± 0.0112
hw.pat.L.mean	0.5995	0.0038 ± 0.0157
PCo3	0.1752	-0.0021 ± 0.0054
fw.pat.VH.mean	0.4878	0.0019 ± 0.0135
hw.shp.rough	0.1854	0.0018 ± 0.0047
fw.pat.L.mean	0.2887	0.0014 ± 0.0058
hw.pat.L.x	0.1802	0.0012 ± 0.0046
fw.pat.E.x	0.2406	0.0012 ± 0.0075
PCo1	0.1950	0.001 ± 0.0031
hw.pat.P.mean	0.1343	-0.0005 ± 0.0038

fw.pat.L.x	0.2393	-0.0003 ± 0.004
fw.col.by.mean	0.2451	0.0002 ± 0.0069
PCo2	0.1347	-0.0001 ± 0.0026

Supplementary Table 8 | SHAP table for sideways-confusion. Variables are ordered by absolute mean SHAP value.

Feature	Node purity	Mean SHAP ± std dev
hw.pat.VH.mean	0.8423	0.0111 ± 0.0272
hw.pat.L.mean	1.1025	0.0054 ± 0.0234
body.length	0.3049	0.0024 ± 0.0104
fw.pat.L.mean	0.7927	0.002 ± 0.0161
hw.pat.P.stdev	0.3445	0.0018 ± 0.0066
hw.shp.rough	0.3436	0.0013 ± 0.0108
PCo3	0.1722	-0.0011 ± 0.0046
hw.pat.DR.mean	0.1333	0.0011 ± 0.0032
fw.pat.VH.mean	0.2764	0.0011 ± 0.0067
hw.pat.L.x	0.2066	0.0008 ± 0.0074
hw.pat.L.stdev	0.3355	0.0007 ± 0.0071
fw.shp.length	0.1267	-0.0001 ± 0.0022
hw.shp.length	0.1788	-0.0001 ± 0.0023
PCo2	0.2653	-0.0001 ± 0.0055

hw.pat.P.x	0.2025	0 ± 0.0048

Supplementary Table 9 | SHAP table for forwards-energy. Variables are ordered by absolute mean SHAP value.

Feature	Node purity	Mean SHAP ± std dev
hw.pat.L.mean	3.7952	0.0081 ± 0.0641
fw.pat.L.mean	2.5395	0.0052 ± 0.0396
fw.pat.E.mean	0.4418	0.0026 ± 0.0099
fw.pat.L.stdev	0.2084	0.0022 ± 0.0079
hw.pat.L.stdev	0.0936	0.0019 ± 0.0051
hw.pat.E.mean	0.0858	0.0011 ± 0.0047
PCo3	0.5321	0.001 ± 0.0057
fw.pat.L.x	0.6294	0.0007 ± 0.0071
hw.pat.P.x	0.0745	0 ± 0.0015

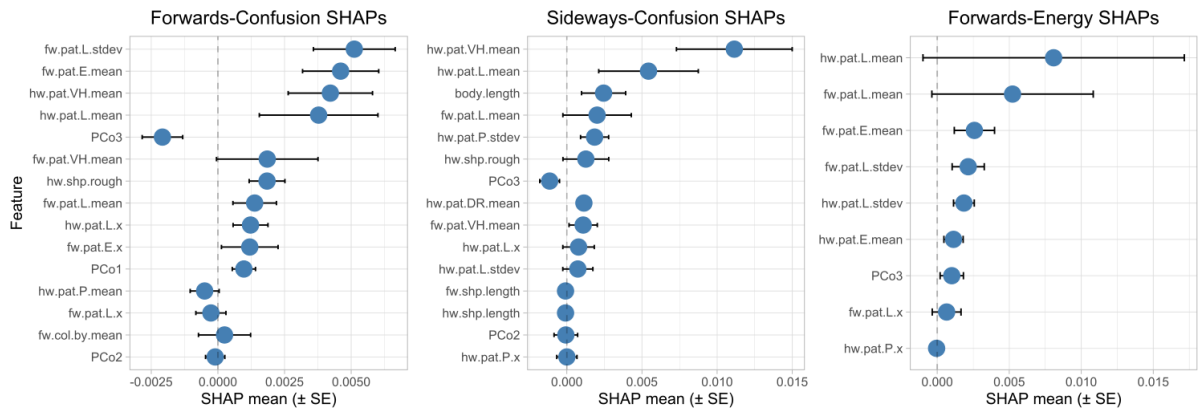

Supplementary Fig.10 | SHAP values for motion confusion metrics, the ranked SHAP values for the reduced forest tree for forwards-confusion, sideways-confusion, and forwards-energy. Positive values indicate instances where the feature increases the motion confusion metric and negative values indicate instances where the variable decreases it.

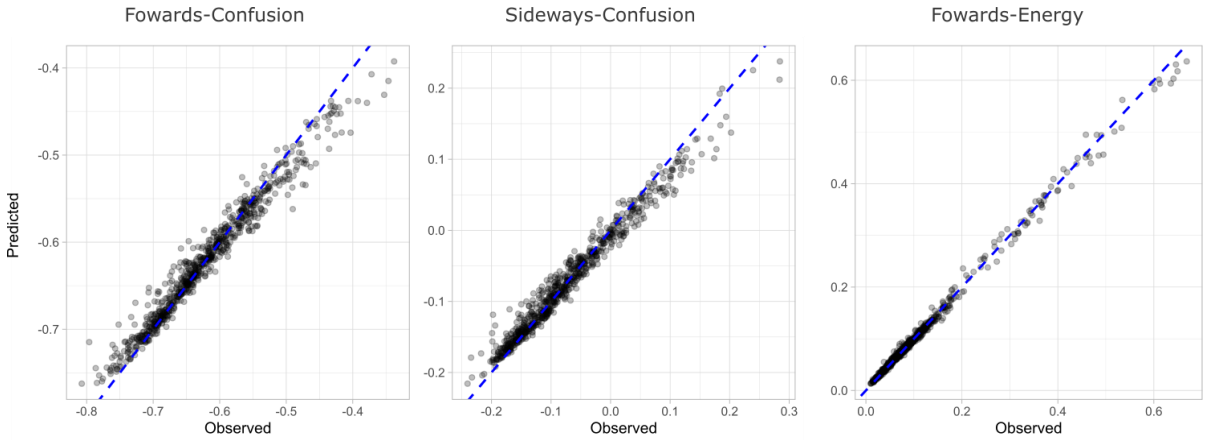

Supplementary Fig.11 | Random forest accuracy plots, the predicted motion confusion values against the observed motion confusion values for forwards-confusion, sideways-confusion and forwards-energy when using our reduced model.

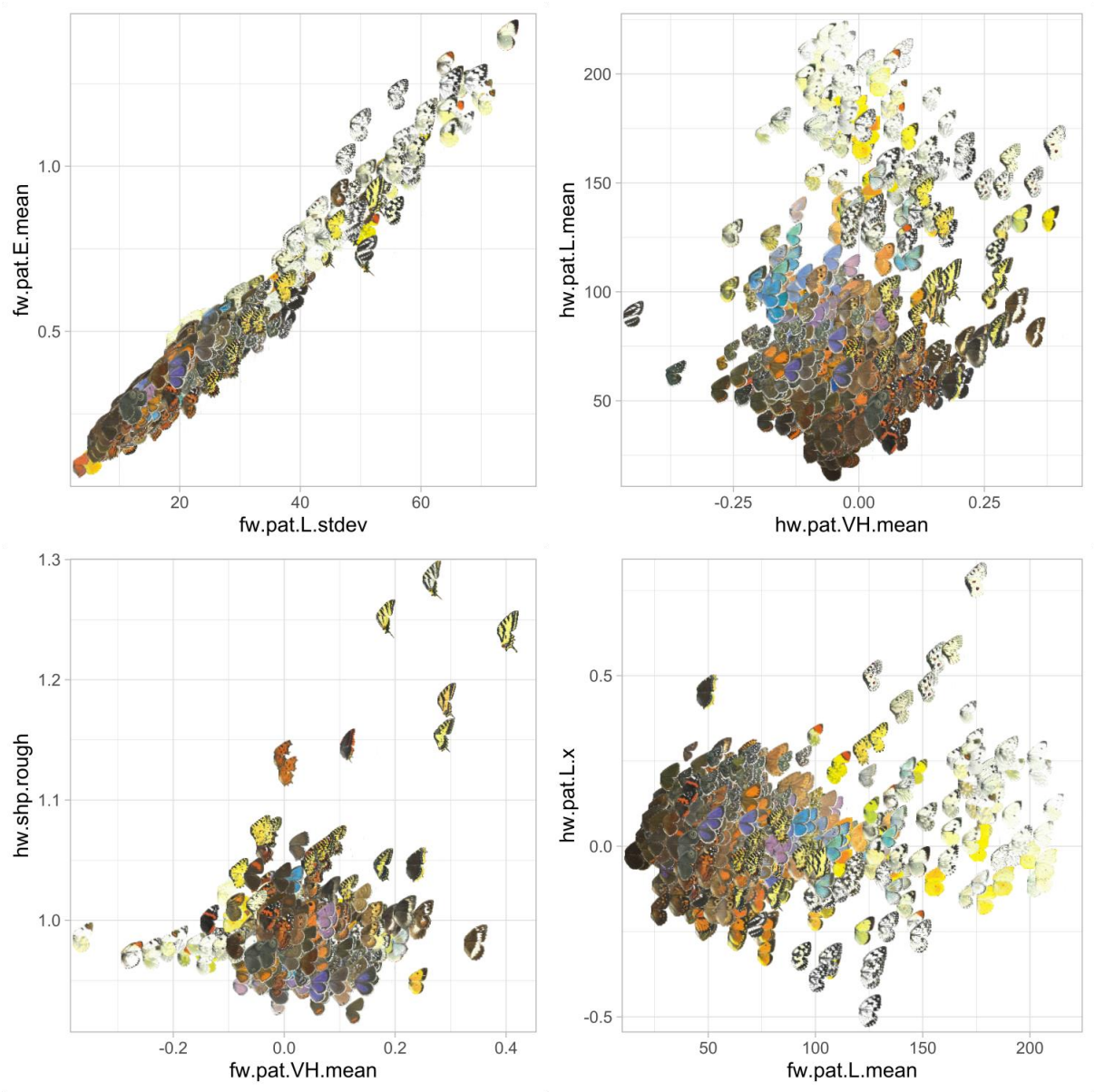

Supplementary Fig.12 | SHAP features for forwards-confusion, shows the top 8 SHAPs for forwards-confusion not including PCos. Each point shows the wing images for the specific butterfly at that point.

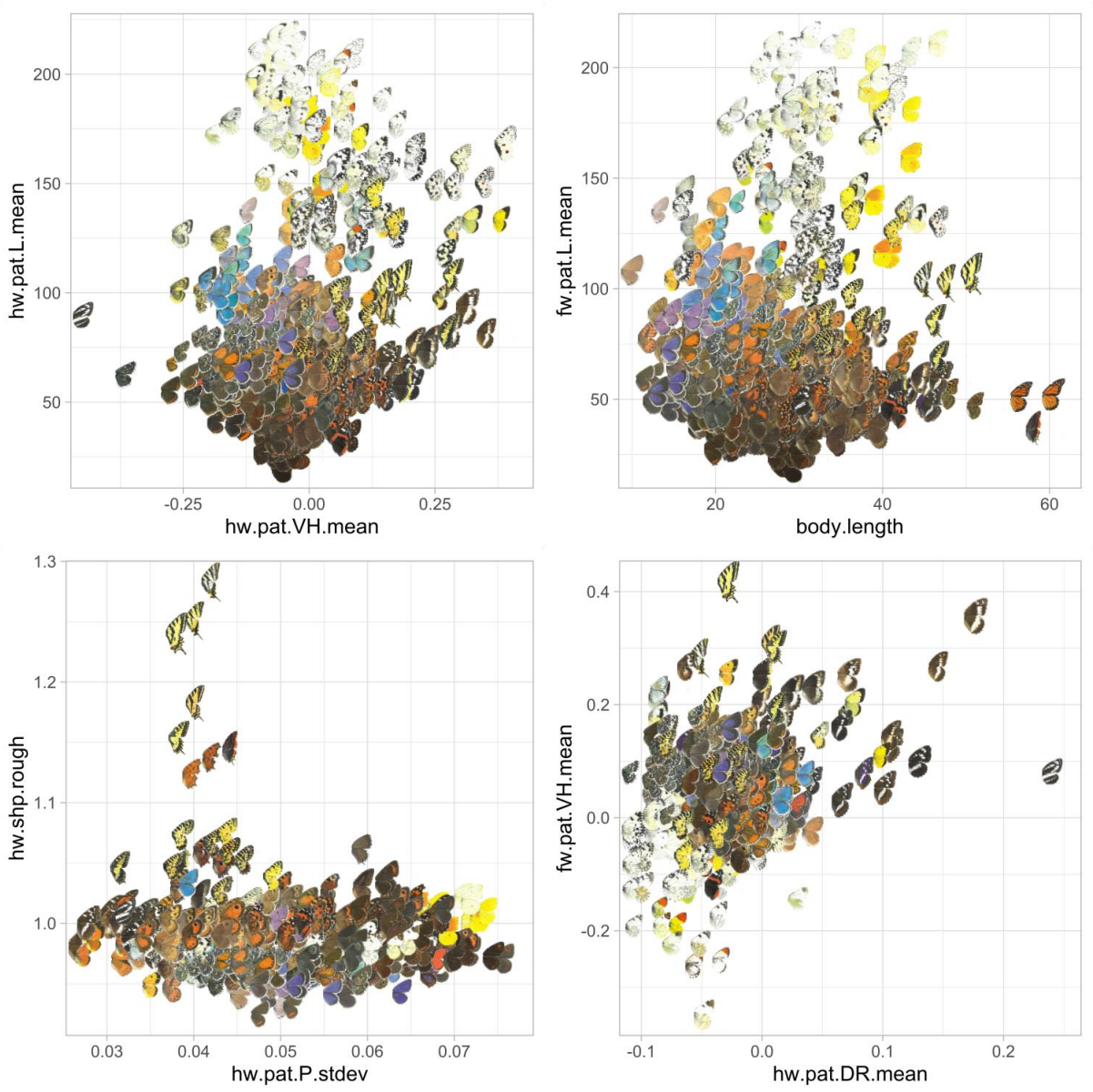

Supplementary Fig.13 | SHAP features for sideways-confusion, shows the top 8 SHAPs for sideways-confusion not including PCos. Each point shows the wing images for the specific butterfly at that point.

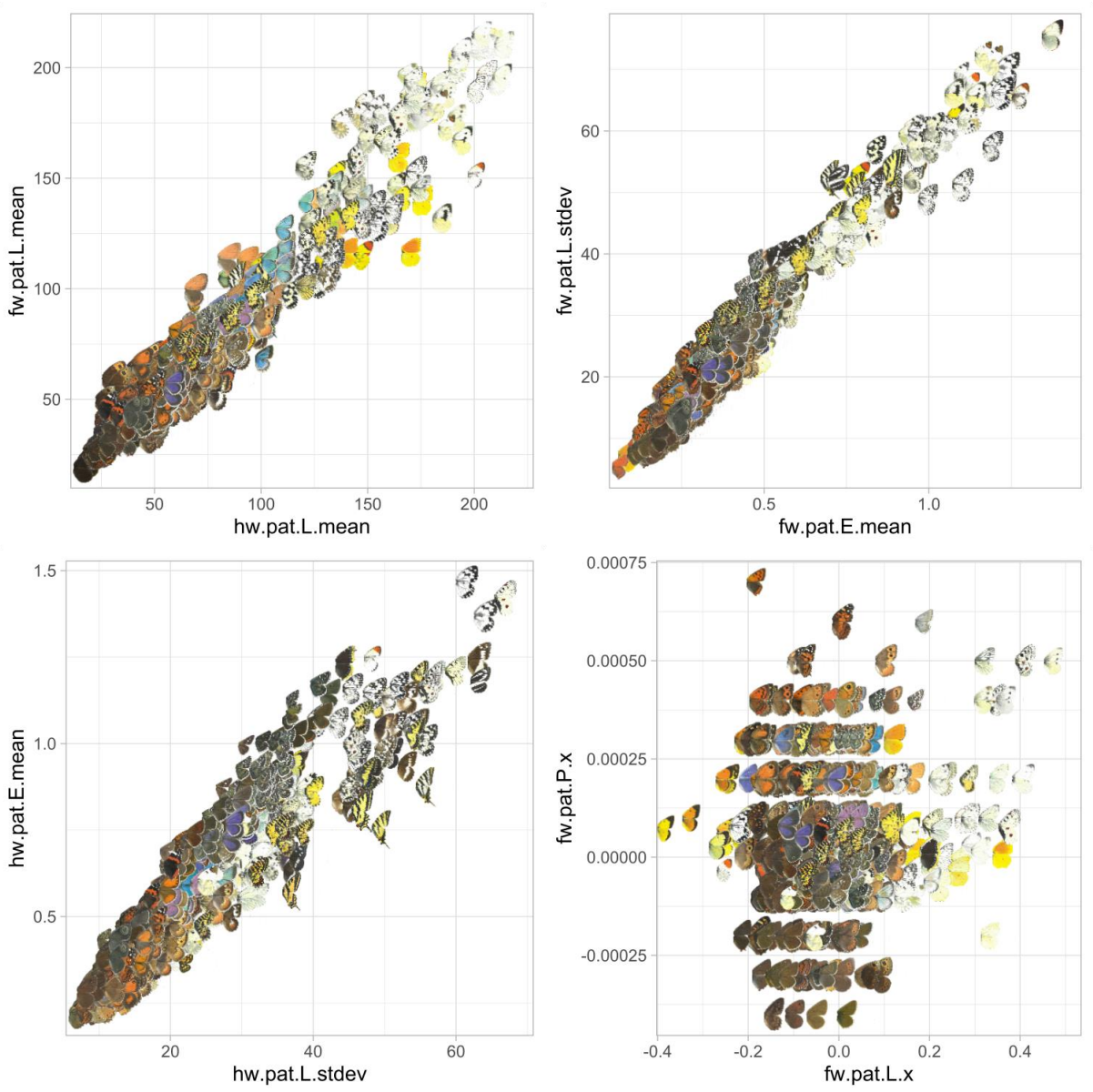

Supplementary Fig.14 | SHAP features for forwards-energy, shows the top 8 SHAPs for forwards-confusion not including PCos. Each point shows the wing images for the specific butterfly at that point.

Butterfly artificial evolution with genetic algorithms

Butterfly pattern generation

Butterfly wing pattern generation was derived from the pattern generator included in the CamoEvo toolbox v2.0 https://github.com/GeorgeHancock471/CamoEvo-v2.0-2022_Plugins. This system uses reaction-diffusion patterns to generate biologically relevant patterns that can be evolved under different selection pressures.

The pattern generator was modified to allow for separate generation of pattern dimensions for the forewing, hindwing and body using masks (see supplementary Fig.15), to add a sin convolution function with different strengths to create eye spot like patterns, two separate colours for the maculation and the background (note butterflies were achromatic for this experiment), and to produce asymmetric edge enhancement patterns (see supplementary Table 10 for full trait list.

Supplementary Table 10 | Gene function table for butterfly pattern generator

Gene Label	Function
dim_for_xcp	Forewing reaction diffusion pattern x coordinate
dim_for_ycp	Forewing reaction diffusion pattern y coordinate
dim_for_wdt	Forewing reaction diffusion pattern selection width
dim_for_asr	Forewing reaction diffusion pattern selection aspect ratio
dim_for_agl	Forewing reaction diffusion pattern rotation
dim_hnd_xcp	Hindwing reaction diffusion pattern x coordinate
dim_hnd_ycp	Hindwing reaction diffusion pattern y coordinate
dim_hnd_wdt	Hindwing reaction diffusion pattern selection width
dim_hnd_asr	Hindwing reaction diffusion pattern selection aspect ratio

dim_hnd_agl	Hindwing reaction diffusion pattern rotation
dim_bod_xcp	Body reaction diffusion pattern x coordinate
dim_bod_ycp	Body reaction diffusion pattern y coordinate
dim_bod_wdt	Body reaction diffusion pattern selection width
dim_bod_asr	Body reaction diffusion pattern selection aspect ratio
dim_bod_agl	Body reaction diffusion pattern rotation
ptn_grd_cvr	Pattern area cover
ptn_grd_sig	Pattern gradient blur
ptn_grd_hgt	Pattern gradient radius
ptn_grd_xps	Pattern gradient x coordinate
ptn_grd_yps	Pattern gradient y coordinate
ptn_grd_sin	Pattern sin convolution, used to produce eye spot like patterns
ptn_bil_sub	Asymmetry noise subtraction before min = 0, for symmetrical patterns just adds noise to pattern shape.
ptn_bil_sig	Asymmetry noise blurring gaussian sigma, for symmetrical patterns just adds noise to pattern shape.
ptn_bil_int	Asymmetry noise intensity level, for symmetrical patterns just adds noise to pattern shape.
ptn_edg_sig	Wing edge, gaussian blur sigma of mask used to shape pattern to wing edge
ptn_edg_rto	Wing edge, ratio between positive and negative
ptn_edg_dfm	Wing edge, reform intensity
eem_int_lvl	Edge enhancement internal intensity level

eem_int_sig	Edge enhancement internal gaussian blur
eem_int_exp	Edge enhancement internal expansion level
eem_int_xst	Edge enhancement internal x offset
eem_int_yst	Edge enhancement internal y offset
eem_ext_lvl	Edge enhancement external intensity level
eem_ext_sig	Edge enhancement external gaussian blur
eem_ext_exp	Edge enhancement external expansion level
eem_ext_xst	Edge enhancement external x offset
eem_ext_yst	Edge enhancement external y offset
col_mc1_lmv	Maculation colour L* 1
col_mc1_rgv	Maculation colour a* 1
col_mc1_byv	Maculation colour b* 1
col_mc2_lmv	Maculation colour L* 2
col_mc2_rgv	Maculation colour a* 2
col_mc2_byv	Maculation colour b* 2
col_bg1_lmv	Background colour L* 1
col_bg1_rgv	Background colour a* 1
col_bg1_byv	Background colour b* 1
col_bg2_lmv	Background colour L* 2
col_bg2_rgv	Background colour a* 2

col_bg2_byv	Background colour b* 2
grd_mac_hgt	Maculation colour gradient radius
grd_mac_sig	Maculation colour gradient sigma
grd_mac_sin	Maculation colour gradient sin
grd_mac_agl	Maculation colour gradient angle
grd_bgd_hgt	Background colour gradient radius
grd_bgd_sig	Background colour gradient sigma
grd_bgd_sin	Background colour gradient sin
grd_bgd_agl	Background colour gradient angle
grd_blr_mac	Background colour gradient radius
spk_nm1_lgt	Speckling 1 light intensity
spk_nm1_drk	Speckling 1 dark intensity
spk_nm1_sig	Speckling 1 gaussian blur
spk_nm1_ycd	Speckling 1 y coordinate
spk_nm2_lgt	Speckling 2 light intensity
spk_nm2_drk	Speckling 2 dark intensity
spk_nm2_sig	Speckling 2 gaussian blur
spk_nm2_ycd	Speckling 2 y coordinate

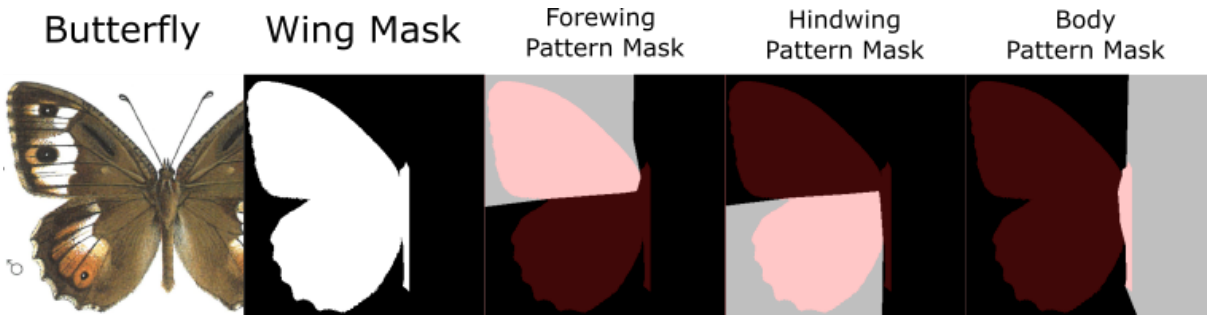

Supplementary Fig.15 | Butterfly wing shape extraction, shows how the wing shape masks and pattern area masks were made for a butterfly using a nymphalid as an example. First the wing was masked and then an area was drawn for the forewing, hindwing and body pattern. Red overlay shows the butterfly wing mask over the mask areas. White indicates a region where patterns are contained within.

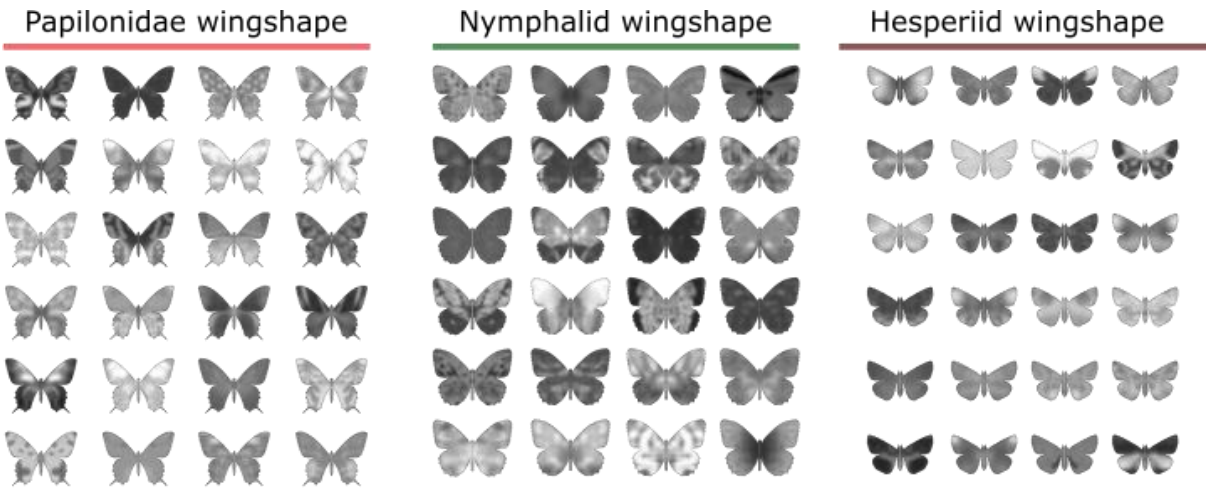

Supplementary Fig.16 | Example wing patterns, shows one whole population (N=24) for each of the three butterfly wing shapes used. All patterns are from the first generation (generation=0) where each of the genes is randomly generated in a uniform distribution from 0-1 for each gene.

ImageGA settings

0
custom
24
20
uniform
fraction
0.6667
0.3333
0
0.001

0.005
0.005
0.33
0.001
0.005
0.005
0.33
0
0
0
0
0
0
0.1
true
true
true
random
1
incomplete
ranked_choice
random
none

Evolved butterfly phenotypes

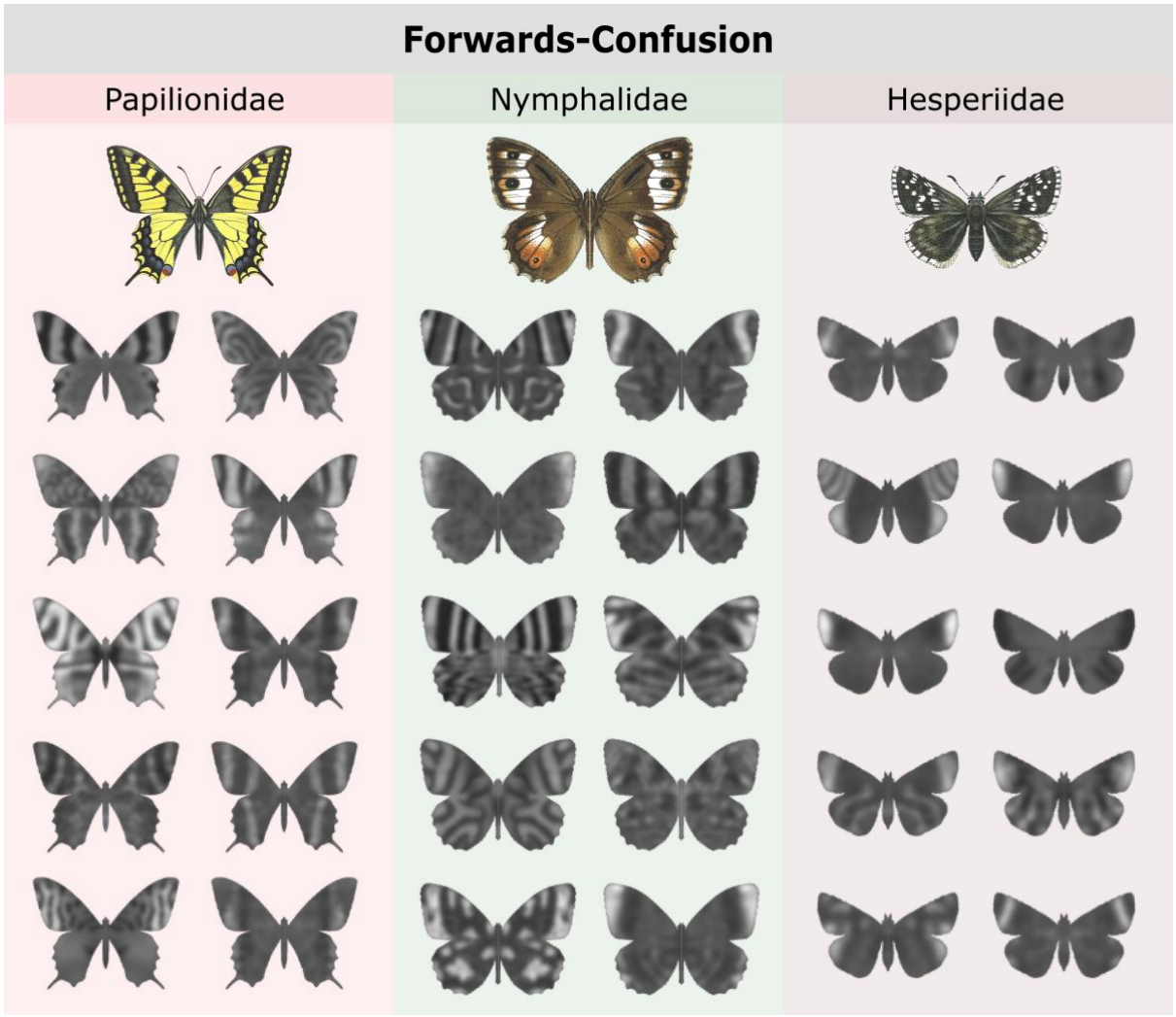

Supplementary Fig.17 | Forwards-Confusion evolved butterflies, showing one individual for each population evolved for forwards-confusion from the final generation (generation=20) and separated by the three wing shapes.

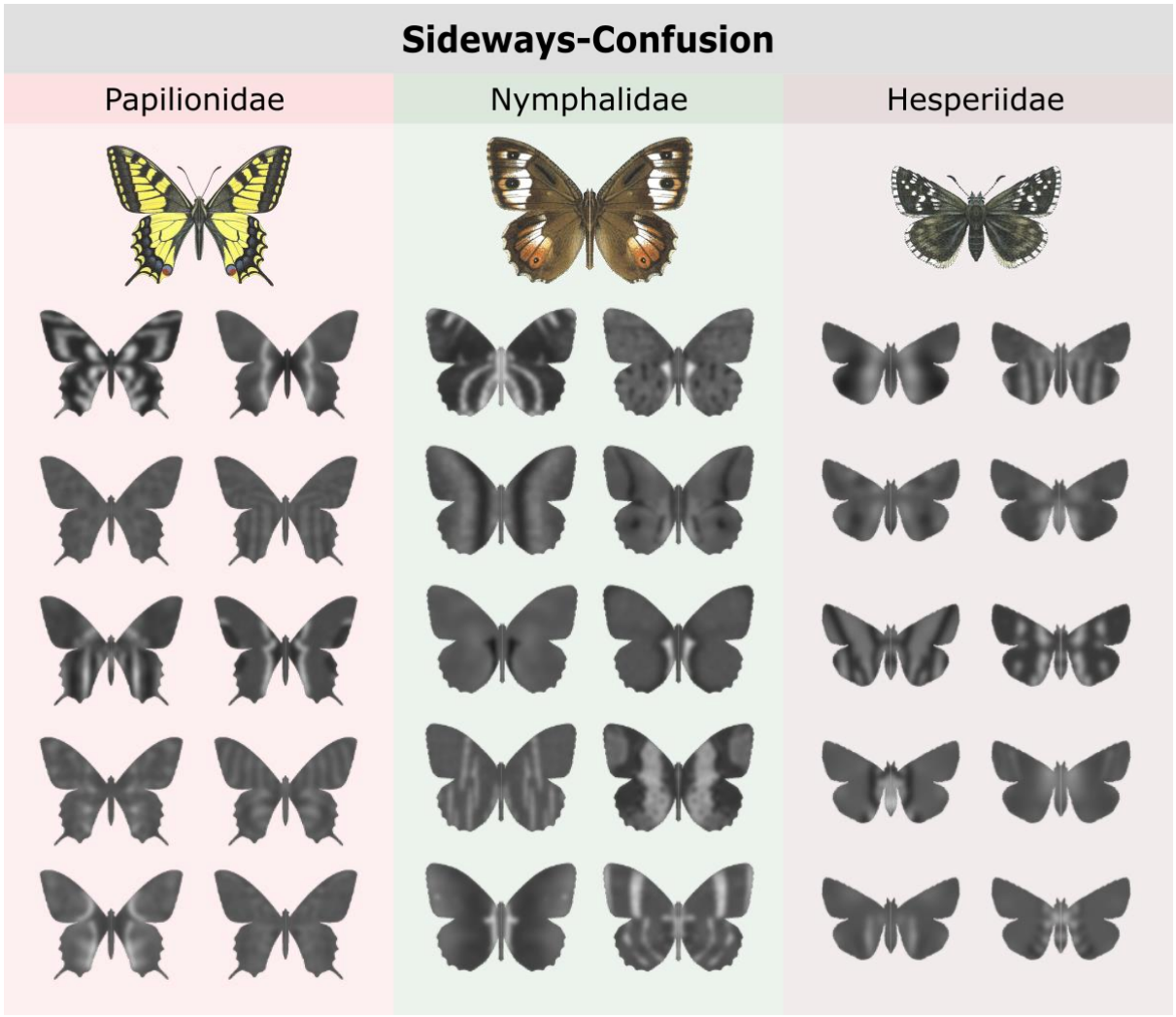

Supplementary Fig.18 | Sideways-Confusion evolved butterflies, showing one individual for each population evolved for sideways-confusion from the final generation (generation=20) and separated by the three wing shapes.

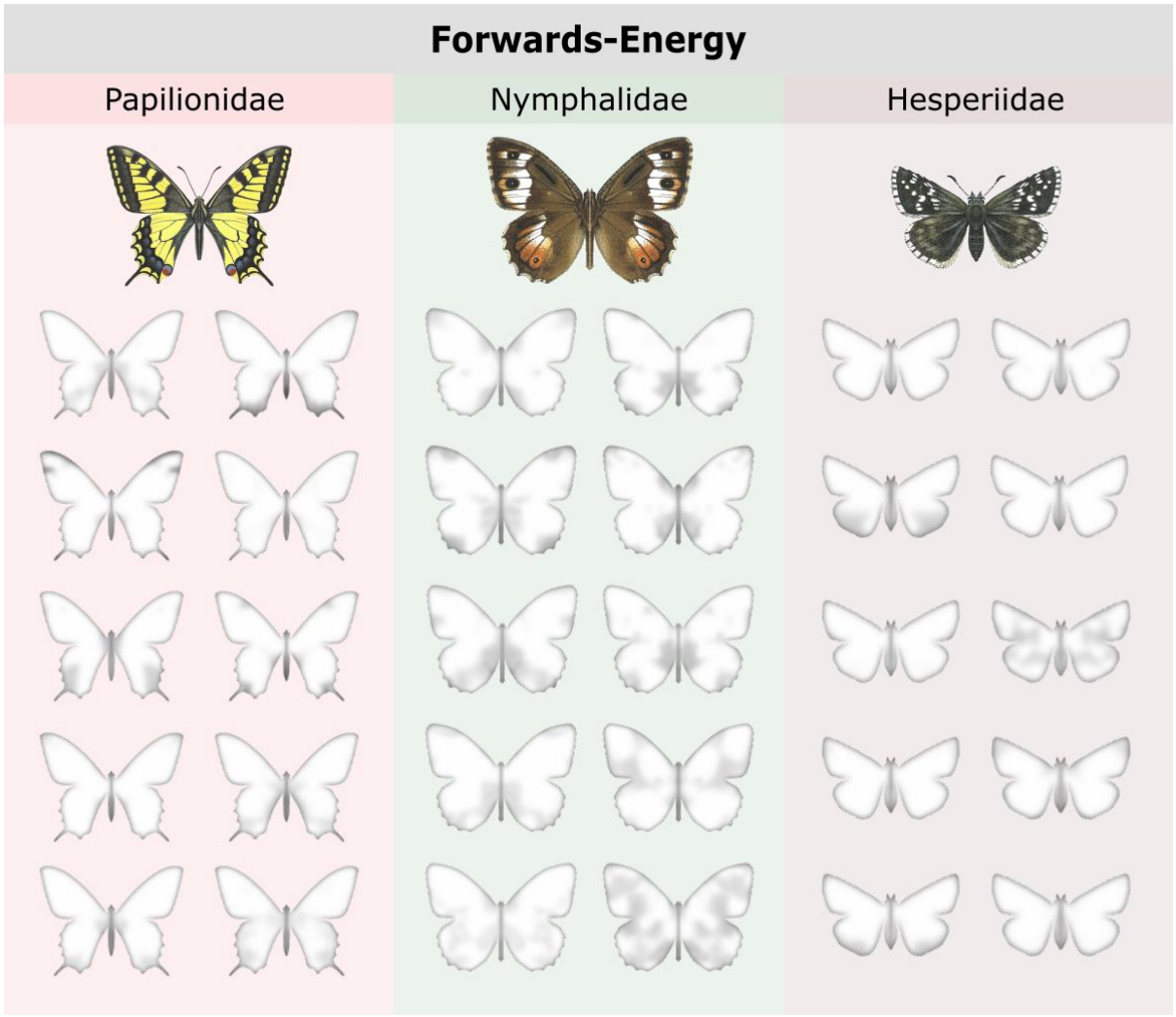

Supplementary Fig.19 | Forwards-Energy evolved butterflies, shows one individual for each population evolved for forwards-energy from the final generation (generation=20) and separated by the three wing shapes.

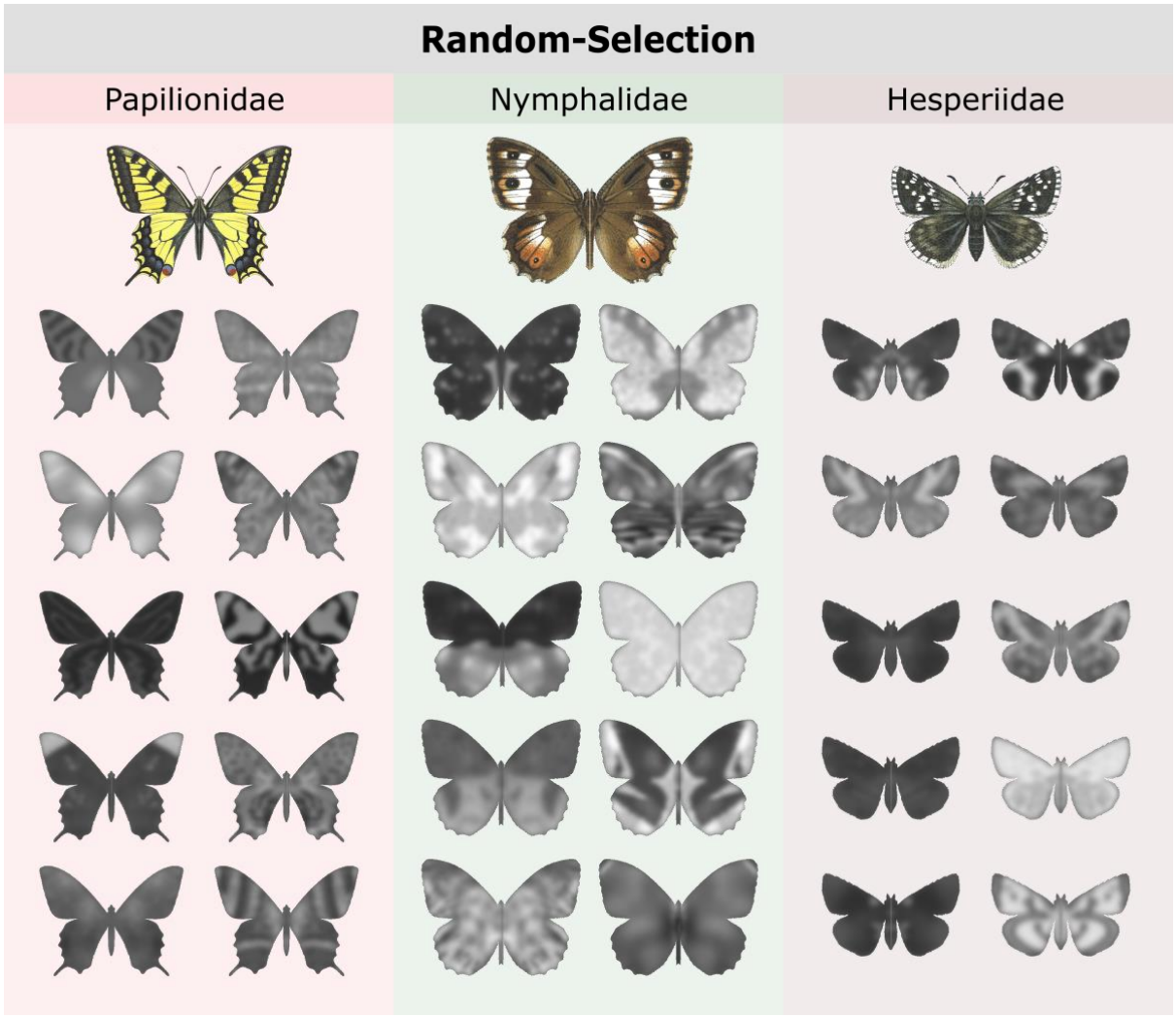

Supplementary Fig.20 | Random-Selection evolved butterflies, showing one individual for each population evolved with randomised fitness values from the final generation (generation=20) and separated by the three wing shapes.

Influence of treatment on motion confusion metrics

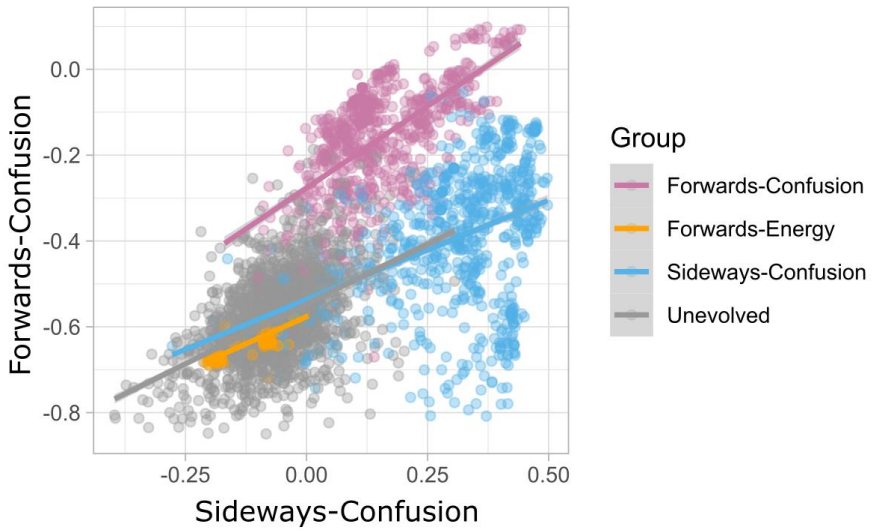

Supplementary Fig.21 | Forwards- and sideways-confusion correlation, shows the linear regression plot for forwards- and sideways-confusion for the unevolved generation 0 butterflies and the final generation 20 for the three different evolution treatments. Butterflies under random-selection were excluded as they weren't measured for EMD.

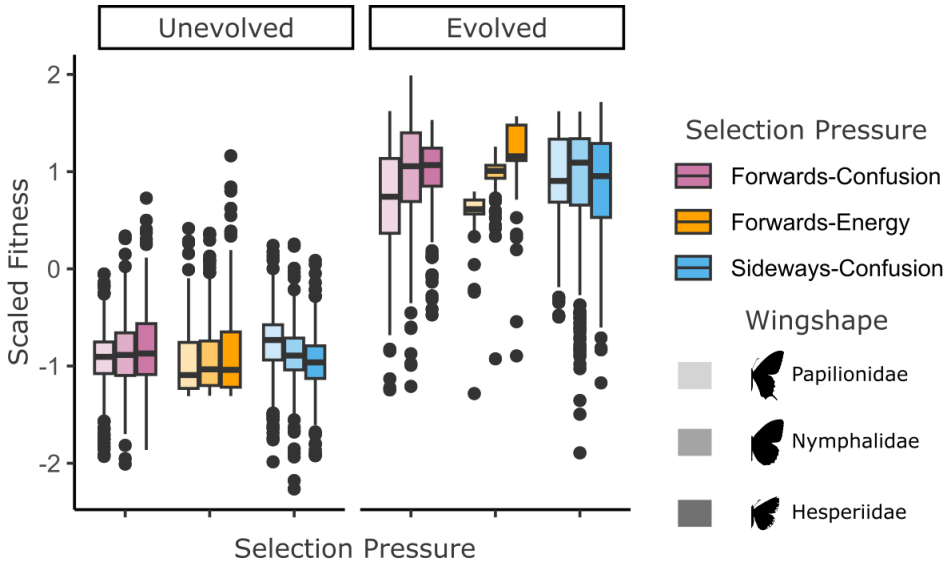

Supplementary Fig.22 | Change in fitness between start and end, shows the scaled (mean = 0, std dev = 1) fitness for the three evolution treatments for the three evolution treatments and separated by wingshape. Left to right and with decreasing luminance are the three wing shapes (Papilonidae, Nymphalidae, and Hesperiidae)

Butterflies significantly improved in fitness across generations for all non-random treatments when tested using a linear model with scaled fitness as the response variable and

generation (start and end) as the predictor variable (end vs start, β = 1.788675, t value = 185.2, SE = 0.010, p <0.001). Butterflies under random-selection were excluded as they weren't measured for EMD.

PCA loadings

Supplementary Table 11 | Ordered image pattern feature loadings for PC1 and PC2 variables are sorted by their absolute contribution. PC1 is primarily pattern contrast on the forewing and hindwing and PC2 is primarily pattern orientation and

PC1		**PC2**	
Feature	***Loading***	***Feature***	***Loading***
fw.pat.DR.stdev	0.268563	hw.pat.OA.x	-0.29989
hw.pat.E.mean	0.267379	hw.pat.VH.x	0.282803
fw.pat.E.mean	0.264071	fw.pat.VH.x	0.278714
fw.pat.VH.stdev	0.263816	hw.pat.OA.stdev	0.258527
fw.pat.OA.stdev	0.263306	fw.pat.L.mean	-0.25602
hw.pat.L.stdev	0.262894	fw.pat.DR.x	0.23709
fw.pat.L.stdev	0.262455	fw.pat.DR.mean	0.23574
hw.pat.VH.stdev	0.258653	hw.pat.DR.stdev	0.209364
hw.pat.DR.stdev	0.258521	fw.pat.P.stdev	0.207509
hw.pat.E.stdev	0.255711	hw.pat.L.mean	-0.20327
fw.pat.E.stdev	0.254993	hw.pat.E.x	0.201842
hw.pat.OA.stdev	0.245247	hw.pat.VH.stdev	0.200999
fw.pat.L.mean	0.181333	fw.pat.L.x	-0.1738
hw.pat.L.mean	0.180075	fw.pat.E.mean	-0.16771
fw.pat.L.x	0.15633	fw.pat.L.stdev	-0.1601
fw.pat.P.stdev	-0.13928	fw.pat.OA.mean	-0.1536
hw.pat.P.stdev	-0.13533	hw.pat.E.stdev	0.151398
hw.pat.P.mean	-0.12265	fw.pat.VH.mean	0.140332

fw.pat.P.mean	-0.12035	hw.pat.E.mean	0.139249
hw.pat.DR.mean	-0.05912	hw.pat.DR.mean	0.12115
fw.pat.E.x	0.055724	hw.pat.DR.x	0.118256
fw.pat.DR.x	0.055361	hw.pat.L.x	0.117725
fw.pat.VH.x	0.0539	hw.pat.P.mean	-0.11541
hw.pat.P.x	0.049861	fw.pat.P.mean	0.114024
hw.pat.OA.mean	-0.04717	fw.pat.E.x	0.112363
hw.pat.OA.x	-0.04444	fw.pat.DR.stdev	-0.09109
fw.pat.DR.mean	-0.04351	fw.pat.OA.stdev	-0.09089
hw.pat.DR.x	0.041132	fw.pat.OA.x	-0.09034
hw.pat.VH.x	0.037225	fw.pat.E.stdev	-0.07976
fw.pat.VH.mean	0.033612	hw.pat.L.stdev	0.070147
hw.pat.L.x	-0.02826	hw.pat.VH.mean	-0.06782
fw.pat.P.x	0.025351	hw.pat.P.stdev	0.062152
fw.pat.OA.x	0.02347	fw.pat.VH.stdev	-0.03231
hw.pat.E.x	0.021196	hw.pat.DR.y	-0.02788
fw.pat.OA.mean	0.01417	fw.pat.OA.y	0.018925
hw.pat.VH.y	0.01213	hw.pat.P.x	-0.01756
hw.pat.E.y	0.009363	hw.pat.E.y	-0.01744
hw.pat.L.y	-0.00881	hw.pat.P.y	0.012326
fw.pat.VH.y	-0.00772	fw.pat.E.y	0.010222
fw.pat.DR.y	-0.00724	hw.pat.OA.mean	-0.00961
fw.pat.L.y	0.002425	hw.pat.VH.y	-0.00776
fw.pat.OA.y	-0.00219	fw.pat.P.x	0.007445
hw.pat.OA.y	-0.0021	hw.pat.OA.y	-0.00628
fw.pat.E.y	-0.00138	fw.pat.P.y	-0.00521
hw.pat.VH.mean	-0.00134	fw.pat.VH.y	-0.00456

fw.pat.P.y	0.001317	fw.pat.DR.y	-0.0044
hw.pat.DR.y	-0.00032	fw.pat.L.y	0.004068
hw.pat.P.y	-0.00031	hw.pat.L.y	-0.00308

Pairwise comparison table

Supplementary Table 12 | Tukey posthoc test for real pairwise comparisons between butterflies (GA generated natural) and all naturally occurring butterflies

Contrast	Estimate	SE	DF	T ratio	P value
Nature vs Unevolved	-0.10241	0.000996	2847828	-102.792	<.0001
Nature vs Forwards-Confusion	0.05566	0.00461	2847828	12.066	<.0001
Nature vs Sideways-Confusion	-0.00096	0.00416	2847828	-0.231	0.9999
Nature vs Forwards-Energy	-0.12157	0.00447	2847828	-27.212	<.0001
Nature vs Random-Selection	-0.06167	0.00454	2847828	-13.589	<.0001
Unevolved vs Forwards-Confusion	0.15806	0.00455	2847828	34.742	<.0001
Unevolved vs Sideways-Confusion	0.10145	0.00409	2847828	24.813	<.0001
Unevolved vs Forwards-Energy	-0.01916	0.0044	2847828	-4.353	0.0002
Unevolved vs Random-Selection	0.04074	0.00447	2847828	9.105	<.0001
Forwards-Confusion vs Sideways-Confusion	-0.05662	0.00608	2847828	-9.308	<.0001
Forwards-Confusion vs Forwards-Energy	-0.17723	0.0063	2847828	-28.14	<.0001
Forwards-Confusion vs Random-Selection	-0.11733	0.00635	2847828	-18.481	<.0001
Sideways-Confusion vs Forwards-Energy	-0.12061	0.00597	2847828	-20.191	<.0001

Sideways-Confusion vs Random-Selection	-0.06071	0.00603	2847828	-10.074	<.0001
Forwards-Energy vs Random-Selection	0.0599	0.00624	2847828	9.593	<.0001

485

486